Overset grid generation with inverse scattering technique for object and crack detection

Deanne Anak Edwin, Shafrida Sahrani, Kismet Anak Hong Ping
Department of Electrical and Electronic Engineering, Faculty of Engineering, Universiti Malaysia Sarawak, Malaysia

Article Info

ABSTRACT

This paper presents the forward backward time stepping (FBTS) technique with finite difference time domain (FDTD) method and overset grid generation (OGG) method was applied for the reconstruction of object and crack detection. Object and crack detection is widely used in structural health monitoring (SHM) application especially in civil structure to detect the buried object and also cracks. The proposed numerical approach has been validated by investigating different kind of ratio of grid size between the main mesh and sub-mesh. Then, the proposed numerical approach is implemented in the analysis of the detection of objects such as concrete blocks and cracks underground. Here, the numerical errors between the actual result and simulated result had been calculated by using relative error. It is shown that the proposed approach has 5.22% error and nearer to the actual value.

This is an open access article under the CC BY-SA license.

Corresponding Author:

Shafrida Sahrani,
Department of Electrical and Electronic Engineering, Faculty of Engineering,
Universiti Malaysia Sarawak,
94300 Kota Samarahan, Sarawak, Malaysia
Email: sshafrida@unimas.my

1. INTRODUCTION

It has always been a concern of public about the buildings and civil structure that had damaged by seismic waves coming from the Sabah earthquake in Malaysia [1]. The tremors created heavy damages and cracks to some school and public buildings, infrastructures and caused landslips. In a worst condition, some of the collapsed buildings are buried under the soil and also some cracks underground that are created during the earthquake. The buried concrete and the crack underground can affect the integrity of the buildings which it causes structural failures and collapses in the future [2]. In addition, this situation can also lead unsafe working environment for the redevelopment of the buildings and infrastructures in the future. Besides, the disaster can create the lining crack on the tunnel can also be dangerous for public especially those cities that have highway tunnel. In this case, it will decrease the stability of the tunnel structure, the safety and reliability of the lining structure and affects the normal use of the tunnel, and endangers the safety of drivers [3]. Therefore, the post-hazard assessments have to be held to ensure the quality and condition of the damaged buildings, infrastructures and lands before continue to use it in the future. The remaining of the collapsed building should be surveyed in order to know the extent of damages and any obvious dangers before any reconstruction happen [2]. The damage of the building and civil structures can be discovered at a very initial stage to avoid any failures that will result in a devastating fatality.

In past years, a number of techniques have been used for the detection of the buried object [4–10]. For example, a research on the detection of underground subsurface layers and buried objects by using a 2D Finite Difference Time Domain (FDTD) model of Ground Penetrating radar (GPR) tomography [6]. The GPR tomography is a method with high resolution ratio, real-time display and flexible to implement for detecting the buried object [6]. It emits the electromagnetic (EM) waves to the ground and receive the backscattered wave to get the image of the underground subsurface layers and buried objects [6]. Due to the effectiveness and flexibility of the method, the researcher used the technique to obtain the depth of the buried object, conductivity and geometry of the buried objects, for examples; pipes, metal bar and strip and cracks under the ground of the subsurface layers. Aside from the GPR method, there is a research by using non-destructive microwave radar to inspect buried object in concrete structures [4]. The objective of the research is to inspect the safety of the inner structures, the position and the estimation of a buried object. In this method, the antenna is transmitting the microwave and will be refracted on a substrate-air boundary and an air-concrete boundary. Then, it will be reflected on the buried object. After that, the wave is refracted again on a concrete-air boundary and an air-substrate boundary and lastly received on the receiver. In [10], the proposed method is based on the effect of a concentrated test mass on the natural frequency that is defined as a stationary mass. The concentrated test mass can be located in different positions of the beam and cannot be separated from the beam. Here, the frequency is calculated by using Timoshenko beam theory.

However, these previous methods have some limitation when it comes to image reconstruction. Firstly, the GPR method determined the buried objects from the reflected wave of the buried objects. Secondly, the non-destructive microwave radar can only get the estimated values for the buried object's parameters and relative permittivity. Thirdly, the method involves three different aspects; the effect of cracks, the effect of the boundary conditions, and to detect location and qualification of cracks when the boundary condition is uncertain. Hence, these methods were not able to provide enough information for the results of the reconstructed image.

In this paper, the Forward Backward Time Stepping (FBTS) technique with FDTD method is proposed to solve the limitation of the previous methods. In FBTS technique [11–13], a broadband microwave signals are utilized to overcome the inverse scattering problem in the time domain [14]. FBTS technique is able to generate image and give beneficial quantitative information of the buried concrete and crack detection such as the locations, sizes, shape and the properties of dielectric of the unknown object [14, 15]. The Overset Grid Generation (OGG) method will be integrated into the algorithm. OGG method is capable to enhance the quality of the image reconstruction and closely describe the building and land structures for the inverse scattering procedure in FBTS technique. Therefore, this paper combines the advantages of both FBTS technique and OGG method in FDTD to develop the efficient numerical method for the image reconstruction in the detection of buried concrete under the soil.

2. FORWARD BACKWARD TIME STEPPING (FBTS) TECHNIQUE

The forward backward time stepping (FBTS) technique is using broadband microwave signals. This technique is used to solve the inverse scattering problem in the time domain. Previously, FBTS technique has been applied for tumor in dispersive breast tissue detection [15–17] and to reconstruct the electrical parameter profiles of scattering object more accurately. FBTS technique can reconstruct images that give the beneficial numerical data about the size, locations, shapes and the internal composition of buried object.

Figure 1 illustrates the setting of a microwave tomography in FBTS inverse scattering problem in 2D view [18]. An unknown scatterer or object is presumed to be buried in a free space. The object is irradiated continuously by M short pulsed waves produced by current sources $s_m(r, t)$ located at $r = r_m^t (m = 1, 2, …, M)$. In FBTS technique [12, 13, 15, 17], the errors of calculated and measured microwave scattering data will be compared in the time domain. Here, the error functional equation of an estimated electrical parameter vector, p includes of permittivity and conductivity is given by:

$$Q(p) = \int_0^T \sum_{m-1}^M \sum_{n-1}^N |v_m(p; r_n, t) - \bar{v}_m(r_n, t)|^2 \, dt \tag{1}$$

where $\bar{v}_m(r_n, t)$ is the measured electric field in the time domain at the receiving position which caused by a pulse that emitted by the transmitter, m meanwhile $v_m(p; r_n, t)$ is the calculated electric field for an assumed electric parameter p, respectively. The gradient of the error functional can be measured using a forward FDTD computation which followed by a corresponding adjoint FDTD computation in which remaining signals at the receiver signified as $[v_m(p; r_n, t) - \bar{v}_m(r_n, t)]$ that is used as equivalent sources at which the time is reversed [19].
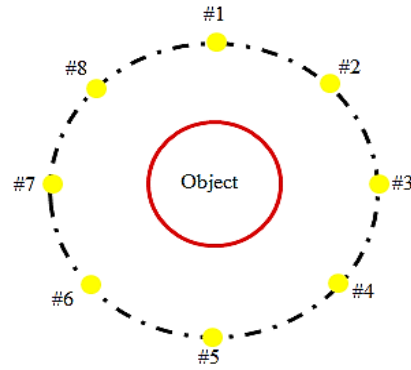
Figure 1. Configuration of microwave tomography for FBTS problem in 2D view [18]

3.   OVERSET GRID GENERATION (OGG) METHOD

Overset Grid Generation (OGG) method is commonly applied in computational fluid dynamics (CFD) [20–23]. This method basically involves of main mesh and a sub mesh that overlapped one another [22]. Every component of the grids in the sub mesh can be measured separately from main mesh. OGG method used bilinear interpolation in order to update and exchange the information of the overlapped data of main mesh and sub mesh [24]. Figure 2 illustrates the algorithm of space and time in FDTD method and Lorentz transformation using OGG method [25]. The electric fields are calculated in both main mesh and sub-mesh separately by using FDTD method.
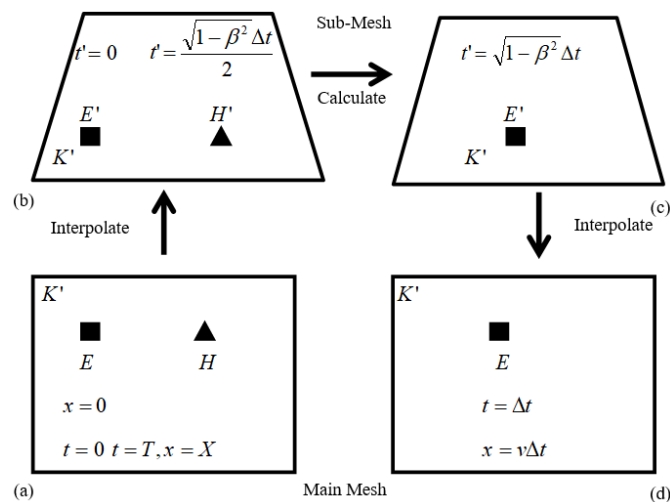

Figure 2. Algorithm of space and time for FDTD method and Lorentz transformation by OGG method [25]

In Figure 2 (a) and Figure 2 (d) show the components of the main mesh, meanwhile in Figure 2 (b) and Figure 2 (c) show the components of the sub-mesh. The components of EM field on the main mesh as shown in Figure 2 (a) are interpolated into the field components in sub-mesh. At this stage, the electric field is measured for both main mesh and sub mesh by using FDTD method. Then, the value of electric field that had been calculated in the sub-mesh as shown in Figure 2 (c) is interpolated back to the main mesh in Figure 2 (d) by Lorentz transformation. Note that, the half time increment is advanced at this stage [25, 26]. In the main mesh, at time $t = \Delta t$ and the value for the components of time for the FBTS technique with FDTD method is:

$$t' = \sqrt{1 - v^2/c^2}\, \Delta t \qquad\qquad (2)$$

so that it can be determined with the leapfrog time-stepping in the FDTD method. It is important to interpolate the time component, $t = T$ at $x = X$ in order to obtain the electric field, E at $t = \Delta t$, $x = v\Delta t$.

As for the sub-mesh, the time increment is half and the components of time for FBTS technique with FDTD method in OGG method is obtained by using:

$$t' = \left(\sqrt{1 - v^2/c^2}\,\Delta t\right)/2 \qquad (3)$$

4. FORWARD BACKWARD TIME STEPPING (FBTS) TECHNIQUE WITH FINITE DIFFERENCE TIME DOMAIN (FDTD) METHOD AND OVERSET GRID GENERATION (OGG) METHOD

In this paper, we integrate FBTS technique with FDTD method into OGG method and applied it in the image reconstruction of the detection of buried object under the soil as shown in Figure 3. First step of the process is the measurement setup for the simulation such as load the original image of buried concrete for simulation and set the coordinates of the buried concrete. The next step is forward-backward time stepping setup. In this step, the position of transmitter and receiver antenna is assigned and all the EM fields are set to zeros as the initial parameter. Note that, the FDTD-OGG algorithm is applied in the FBTS simulation.
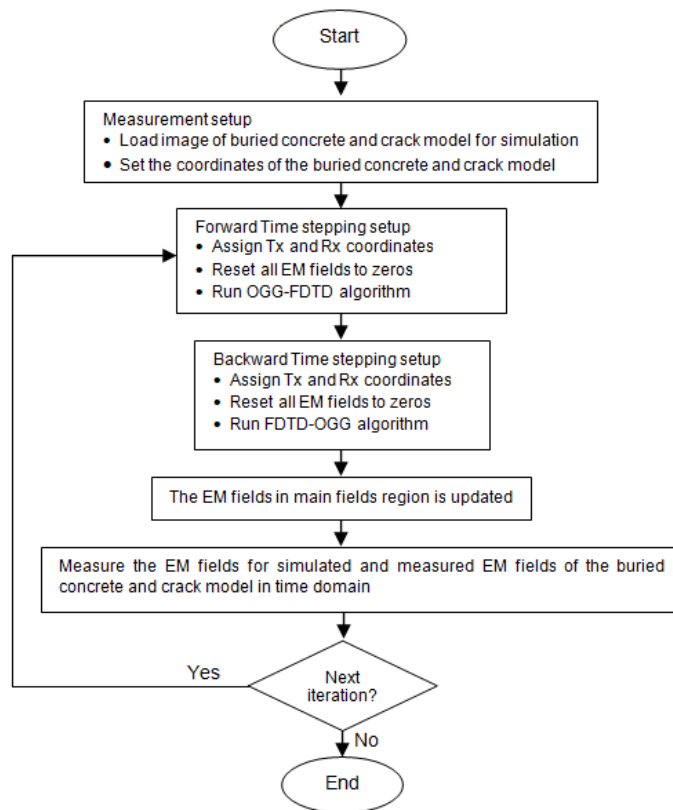
Figure 3. Flow chart for the image reconstruction of detection of buried object and crack detection

In the FBTS main field region, the time component for the is set as $t = t + \Delta t$ while the components of time in FDTD-OGG algorithm is set as $t = t + \Delta t/2$ in order for the time component on the main mesh to be measured and interpolated onto the sub-mesh. The time step that is chosen in this analysis need to satisfy the Courant condition $c \leq \Delta x / \Delta t$, where c is the velocity of light, $c = 2.998 \times 10^8\ m/s$ [27]. In the FDTD-OGG algorithm, the point of the grid for the sub-mesh that overlapped with the main mesh is identified. Here, both of the main mesh and sub-mesh are remained stationary. Next, the components of EM field on the main mesh are interpolated into sub-mesh. Here, the electric field for both main mesh and sub-mesh are calculated through FDTD method. Then, the electric field's value that had been calculated in the sub-mesh is updated into main fields region. The whole previous procedure is repeated to measure the magnetic field. The last step of the process, the EM fields for simulated and measured EM fields of the buried concrete in time domain are calculated. The entire process is repeated until the time stepping is finished.

5. RESULTS AND ANALYSIS

5.1. Numerical setup for buried concrete detection by using FBTS technique with FDTD method and OGG method

Figure 4 demonstrates the numerical modelling of the buried object by using FBTS technique with FDTD method and OGG method on the overlapped main mesh. The grid's number for main mesh $I_{m(m)} \times I_{m(n)}$ is set to 190×190 and the number of grids for sub-mesh $I_{s(i)} \times I_{s(j)}$ is set into 40×20. The length of the main mesh and sub-mesh are fixed, where $L_m = 0.20\,m$ and $L_s = 0.05\,m$ respectively. In this simulation, Δt is set to $2.3115 \times 10^{-12}(s)$ and it satisfied the Courant condition. Here, 16 antennas are surrounded around the region of interest (ROI). The measurement is repeated until the number of antennas utilized. The distance between each of the antennas is set as $170\,mm$. All these grids will be terminated by the Convolutional Perfectly Matched Layer (CPML) [28–30]. The outer boundary of the main mesh is the CPML with the thickness of $15\,mm$.
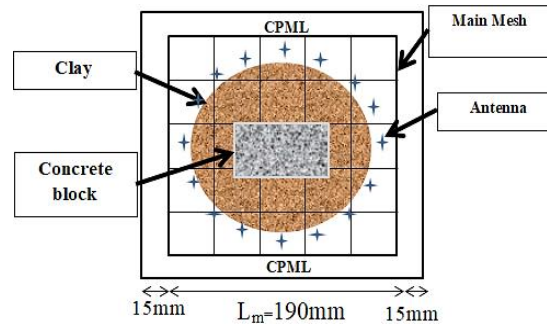

Figure 4. Numerical model of buried concrete by using FBTS technique with FDTD method and OGG method

A sinusoidally modulated Gaussian pulse is applied as excitation signal with a center bandwidth, $f_c = 2.0\,GHz$. The space increment of the grid for main mesh, Δx_m and Δy_m is set to $1\,mm$. As the ratio of grid size is $R = 1.0$, Δx_s, Δy_s are set to be equivalent to Δx_m, Δy_m. The radius of ROI is set to 50 mm. Here, the sub-mesh is set as a concrete block. The circular region of interest is replaced with the clay region. The background medium is set as free space in order the equipment is easier to be maintained. In this analysis, a concrete is assumed to be immersed in clay region. The length and the width of the concrete is set as $40\,mm$ and $20\,mm$ respectively. The embedded sub mesh is positioned at the center of the main mesh with $x_x = 90$, $y_x = 100$. The relative permittivity value for the concrete is set to $\varepsilon_r = 6.7$ while the region of interest is set as $\varepsilon_r = 12.0$.

5.1.1. Image Reconstruction of the detection of buried concrete block using FBTS technique with FDTD method and OGG method

Figure 5 (a) illustrates the actual image of relative permittivity reconstruction for a concrete which is assumed to be immersed in clay region. The length and the width of the concrete is set as $40\,mm$ and $20\,mm$ respectively. The embedded sub mesh is fixed at the centre of the main mesh with $x_x = 90$, $y_x = 100$. Figure 5 (b) shows the image after the reconstruction for the relative permittivity. Figure 5 (c) shows the cross-section of relative permittivity of the reconstruction image.

The solid line shows the actual result while the dashed line is the simulated result. From this result, it is observed that the concrete block is able to be detected and reconstructed. The comparison of the numerical analysis between the actual value and the simulated value is shown in Table 1. The actual value and simulated result for cross-sectional view of reconstructed relative permittivity from Figure 5 (c) are compared as shown in Table 1. The numerical errors between the actual result and simulated result had been calculated by using relative error as in (4).

$$Relative\ Error = |E_z(t) - E_0(t)|/E_0(t) \qquad (4)$$

The percentage of the numerical errors between both results is 5.22%. Therefore, it is shown that the reconstructed image of the buried object able to detect and nearly to the actual value.
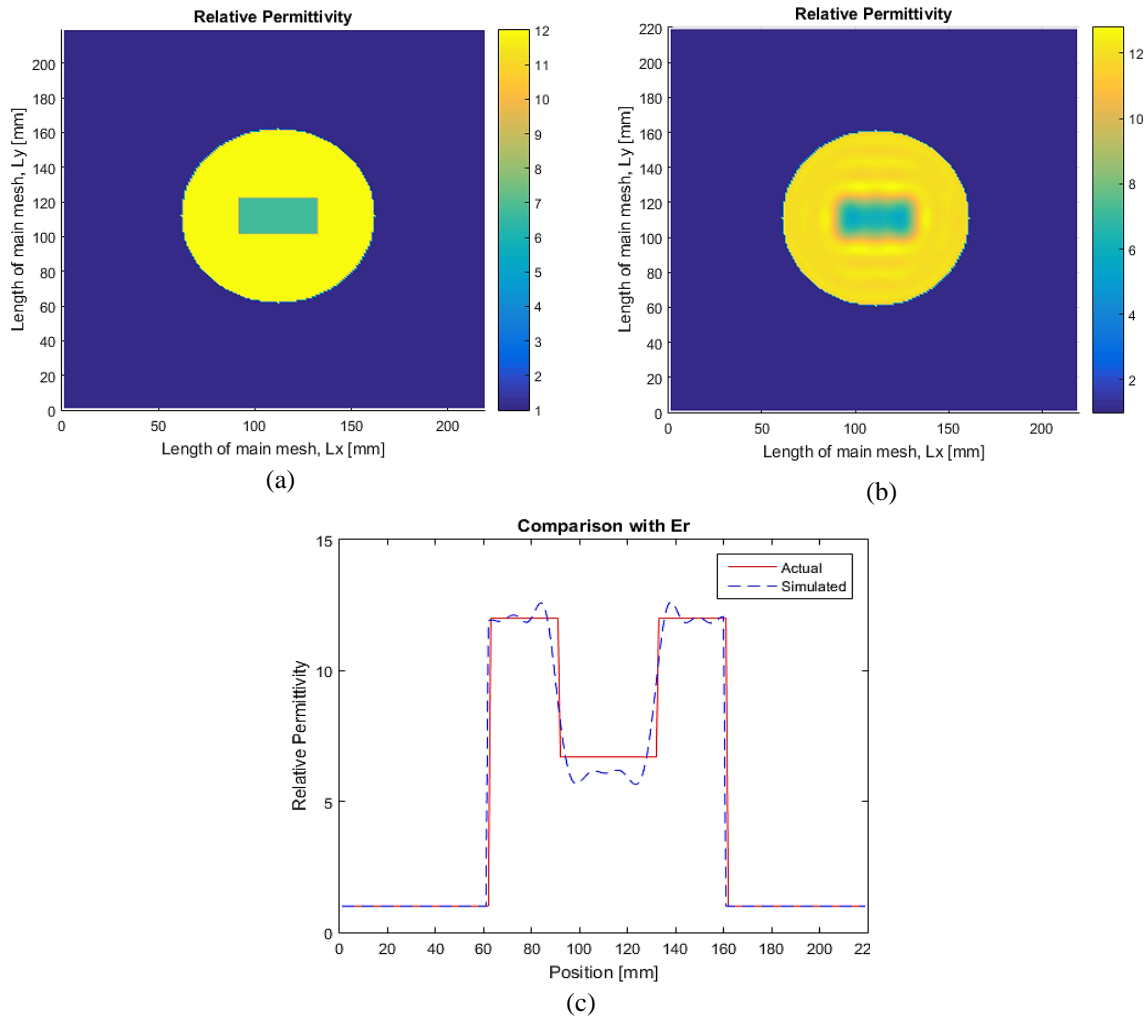
Figure 5. Image Reconstruction of the detection of buried concrete block using FBTS technique with FDTD method and OGG method: (a) Actual image of relative permittivity, (b) Reconstructed image of relative permittivity, (c) Cross-sectional view of reconstructed image relative permittivity

Table 1. Error analysis of actual result and simulated result for relative permittivity value

	Actual Value	Simulated Result
Relative Permittivity (The highest value)	12.0	12.6269
Percentage of Relative Error (%)		5.22%

5.2. Numerical setup for crack detection by using FBTS technique with FDTD method and OGG method

Figure 6 illustrates the numerical model for the crack detection underground by using FBTS technique with FDTD method and OGG method on the overlapped main mesh. A similar setting as the numerical model in Figure 4 is to be applied in this simulation. A random shape crack is assumed to be added in clay region. The relative permittivity (ε_r) value for the sub-mesh is set to $\varepsilon_r = 1.0$ while the ROI is set as $\varepsilon_r = 12.0$. All these grids will be terminated by the CPML.

The outer boundary of the main mesh is the CPML with the thickness of $15\ mm$. The increment of space between the main mesh and sub-mesh is $\Delta x_m = \Delta y_m = \Delta x_s = y_s = 1.0\ mm$. The ratio of grid size between the main mesh and sub-mesh is given by $R = 1.0$. Here, each of the 16 points was used as transmitter sequentially to transmit the EM wave at a time into the clay region to illuminate the crack while the others antennas act as receiver to gather the scattered signal. The measurement is repeated until the number of antennas utilized. The distance between each of the antennas is set as $170\ mm$. A sinusoidally modulated Gaussian pulse is applied as excitation signal with a center bandwidth, $f_c = 2.0\ GHz$.
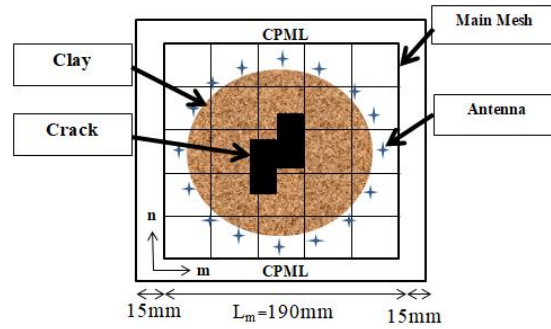
Figure 6. Numerical Model of crack detection by using FBTS technique with
FDTD method and OGG method

5.2.1. Image reconstruction of the crack detection using FBTS technique with FDTD method and OGG method

Figure 7 (a) demonstrates the actual image of relative permittivity reconstruction of a crack is assumed to be added in clay region. The relative permittivity (ε_r) value for the sub-mesh is set to $\varepsilon_r = 1.0$ while the ROI is set as $\varepsilon_r = 12.0$. Figure 7 (b) shows the image after the reconstruction for the relative permittivity. Figure 7 (c) illustrates the cross-section of relative permittivity of the reconstruction image. The solid line shows the actual result while the dashed line is the simulated result. From this result, it is observed that the relative permittivity of the crack can be identified and reconstructed.
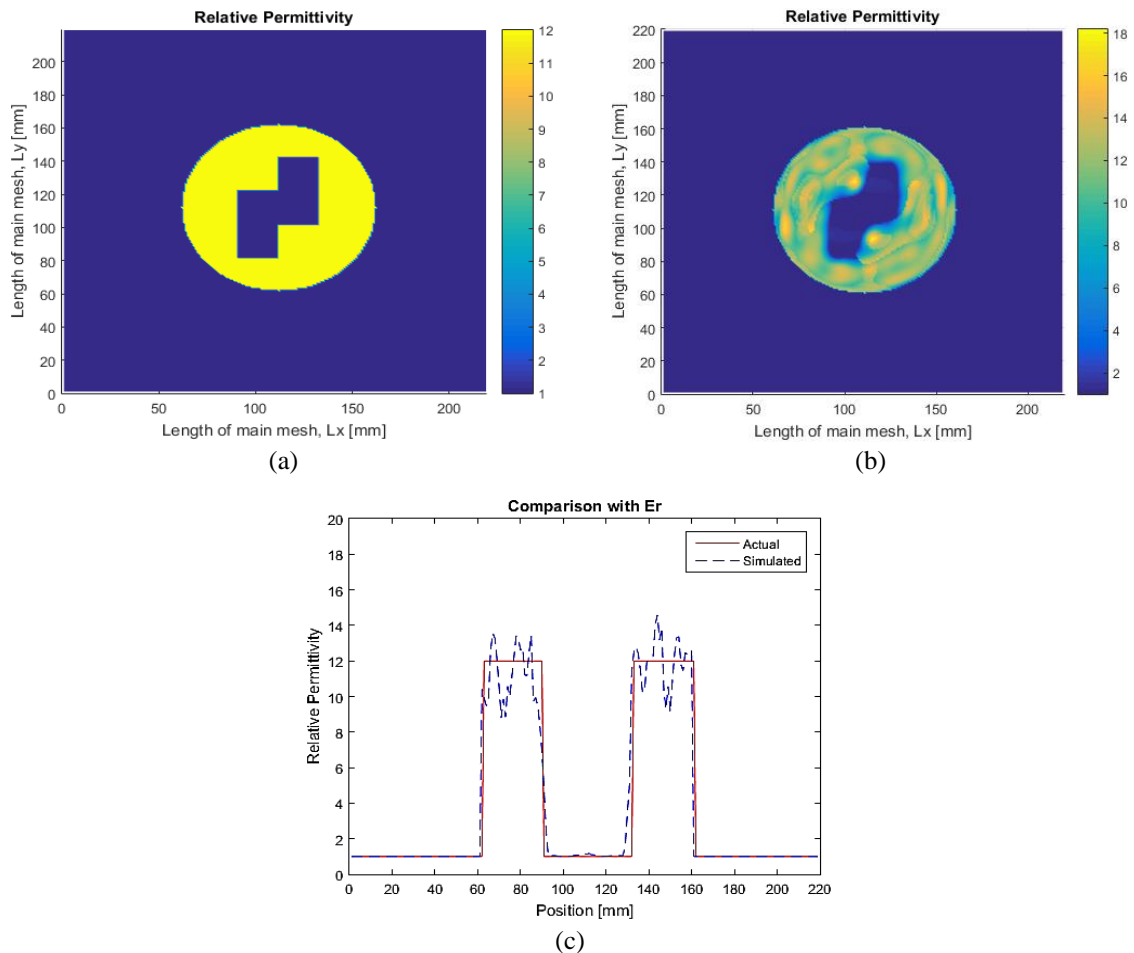

(a)

(b)

(c)

Figure 7. Image Reconstruction of the crack detection using FBTS technique with FDTD method and OGG method: (a) actual image of relative permittivity, (b) reconstructed image of relative permittivity, (c) cross-sectional view of reconstructed image relative permittivity

The comparison of the actual value and simulated results for cross-sectional view of reconstructed relative permittivity from Figure 7 (c) is shown in Table 2. The numerical errors between the actual result and simulated result had been calculated by using relative error as in (4). The percentage of the numerical errors between both results is 21.55%. The percentage of error in this analysis is higher than the analysis in section 5.1.1 due to the limitation of bilinear interpolation in the image reconstruction for irregular shape of the object. However, it can be observed that the reconstructed image of the crack detection is able to reconstruct clearly.

Table 2. Error analysis of actual result and simulated result for relative permittivity value

	Actual Value	Simulated Result
Relative Permittivity (The highest value)	12.0	14.5865
Percentage of Relative Error (%)		21.55%

6. CONCLUSION

In this paper, the proposed numerical approach is further investigated on detection of buried object and crack detection. The image reconstruction of the detection of the buried objects such as concrete and also the crack detection shows that the FBTS technique with FDTD method and OGG method are able to be identified and reconstructed. The outcomes in this paper for the application of detection of crack and buried object have only examined for the case of ratio of grid size between the sub-mesh and main mesh, $R = 1.0$ because it is more stable and has potential in image reconstruction for the detection of the unknown object.

ACKNOWLEDGEMENTS

REFERENCES

[1] Muguntan Vanar, Ruben Sario and Stephanie Lee, "Strong Earthquake strikes Sabah. The Star Online," [Online], Available: https://www.thestar.com.my/news/nation/2015/06/05/sabah-quake/, 2015.
[2] Farrar C. R., Worden K., "An Introduction to Structural Health Monitoring," *Philoshopical Transactions of The Royal Society A*, vol. 365, no. 1851, pp. 303-315, 2006, doi:10.1098/rsta.2006.1928.
[3] Zhang N., Zhu X., Ren Y., "Analysis and Study on Crack Characteristics of Highway Tunnel Lining," *Civil Engineering Journal,* vol. 5, no. 5, pp. 1119–1123, 2019.
[4] Kubo M., Okamoto M., Takayama J., "Non-destructive inspection of buried object in concrete structures based on improved propagation path model using microwave radar," *2017 56th Annual Conference of the Society of Instrument and Control Engineers of Japan (SICE)*, pp. 695–698, 2017.
[5] R. M. Narayanan, "Through wall radar imaging using UWB noise waveforms," *2008 IEEE International Conference on Acoustics, Speech and Signal Processing*, pp. 5185-5188, 2008.
[6] Y. Liu and L. Guo, "FDTD investigation on GPR detecting of underground subsurface layers and buried objects," *2016 IEEE MTT-S International Conference on Numerical Electromagnetic and Multiphysics Modeling and Optimization (NEMO)*, pp. 1-2, 2016.
[7] Tavakoli M. J., Mallahzadeh A. R., "Wideband Directional Coupler for Millimeter Wave Application based on Substrate Integrated Waveguide," *Emerging Science Journal,* vol. 2, no. 2, pp. 93–99, 2018.
[8] Razian S. A., Mohammadi H. M., "Optimizing Raytracing Algorithm Using CUDA," *Italian Journal of Science & Engineering*, vol. 1, no. 3, pp. 167–178, 2017.
[9] Kouhdaragh M., "Experimental Investigation of Damage Detection in Beam Using Dynamic Excitation System," *Civil Engineering Journal*, vol. 3, no. 10, pp. 920–928, 2017.
[10] Mohtasebi S. M., Khaji N., "An Analytical Method for Crack Detection of Beams with Uncertain Boundary Conditions by a Concentrated Test Mass," *Civil Engineering Journal*, vol. 4, no. 7, pp. 1629–1645, 2018.
[11] Takenaka T., Jia H., Tanaka T., "Microwave Imaging of Electrical Property distributions by a forward-backward time-stepping method," *Journal of Electromagnetic Waves and Applications,* vol. 14, no. 12, pp. 1609–1626, 2000.
[12] Takenaka T., Jia H., Tanaka T., "An FDTD approach to the time domain inverse scattering problem for a lossy cylindrical object," *2000 Asia-Pacific Microwave Conference-Proceedings (Cat. No.00TH8522)*, pp. 365–368, 2000.
[13] Tanaka T., Kuroki N., T. Takenaka, "Filtered forward–backward time-stepping method applied to reconstruction of dielectric cylinders," *Journal of Electromagnetic Waves and Applications*, vol. 17, no. 2, pp. 253–270. 2003.
[14] J. E. Johnson, T. Takenaka and T. Tanaka, "Two-Dimensional Time-Domain Inverse Scattering for Quantitative Analysis of Breast Composition," *IEEE Transactions on Biomedical Engineering*, vol. 55, no. 8, pp. 1941-1945, 2008.

[15] Takenaka T., Moriyama T., Hong Ping K. A., Yamasaki T., "Microwave breast imaging by the filtered forward-backward time-stepping method," *2010 URSI International Symposium on Electromagnetic Theory (EMTS)*, pp. 946–949, 2010.

[16] Hong Ping K. A., Moriyama T., Takenaka T., Tanaka T., "Two-dimensional Forward-Backward Time-Stepping approach for tumor detection in dispersive breast tissues," *2009 Mediterrannean Microwave Symposium (MMS)*, pp. 1–4, 2009.

[17] Johnson J. E., Zhou H., Takenaka T., "Experimental three-dimensional time-domain reconstruction of dielectric objects for breast cancer detection," *Mediterrannean Microwave Symposium,* pp. 423–426, 2006.

[18] Hong Ping K. A., Moriyama T., Takenaka T., Tanaka T., "Reconstruction of Breast Composition in a Free Space Utilizing 2-D Forward-Backward Time-Stepping for Breast Cancer Detection," *4th IET International Conference on Advances in Medical, Signal and Information Processing-MEDSIP* 2008, pp. 1–4, 2008.

[19] H. Harada, D. J. N. Wall, T. Takenaka and M. Tanaka, "Conjugate gradient method applied to inverse scattering problem," *IEEE Transactions on Antennas and Propagation*, vol. 43, no. 8, pp. 784-792, Aug 1995.

[20] Allen C. "CHIMERA volume grid generation within the EROS code," *Proceedings of the Institution of Mechanical Engineers Part G Journal of Aerospace Engineering,* vol. 214, no. 3, pp. 125–141, 2000.

[21] Ferziger J. H., Peric M., "Computational Methods for Fluid Dynamics," Springer, 2002.

[22] Joseph J. S. Shang., "Computational Electromagnetic-Aerodynamics," Wiley-IEEE Press. 2016.

[23] Steger J. L., Benek J. A., "On the use of composite grid schemes in computational aerodynamics," *On the use of composite grid schemes in computational aerodynamics,* vol. 64, no. 1–3, pp. 301–320, 1987.

[24] Iwamatsu H., Kuroda M., "Over Set Grid Generation Method Coupled with FDTD Method while Considering the Doppler Effect," *IEEJ Transactions on Fundamentals and Materials,* vol. 129, no. 10, pp. 699–703, 2009.

[25] Sahrani S., Iwamatsu H., Kuroda M., "A Novel Approach for the Analysis of Electromagnetic Field with Rotating Body," *Applied Computational Electromagnetics Society Journal,* vol. 26, no. 8, pp. 651–659, 2011.

[26] Sadiku M. N. O., "Numerical Techniques in Electromagnetics," CRC Press, 2000. DOI: 10.1201/9781420058277

[27] Taflove A, Hagness S. C., "Computational Electrodynamics: The Finite-difference Time-domain Method," 3rd Edition, Artech House," 2005.

[28] Gedney S. D., "Introduction to the Finite-Difference Time-Domain (FDTD) Method for Electromagnetics," *Synthesis Lectures on Computational Electromagnetics,* Morgan & Claypool Publishers, vol. 6, no. 1, 2011.

[29] Alan Roden J., Gedney S. D., "Convolution PML (CPML): An Efficient FDTD Implementation of the CFS-PML For Arbitrary Media," *Microwave and Optical Technology Letters*, vol. 27, no. 5, pp. 334–339, 2000.

[30] Kunz K. S., Luebbers R. J., "The finite difference time domain method for electromagnetics," CRC Press. 2019. ISBN: 9780849386572.